# *Kepler*: A Brief Discussion of the Mission and Exoplanet Results

WILLIAM J. BORUCKI
Space Scientist
Astrobiology and Space Research Directorate
Ames Research Center, NASA

## Introduction

The *Kepler* Mission was a PI-led NASA Discovery mission designed to determine the frequency of Earth-size and larger planets in the habitable zone (HZ) of other stars (i.e., exoplanets); characterize those planets; and explore the diversity of planetary systems. To accomplish these goals, the Mission was designed to find thousands of planets around various star types assuming that planetary systems were common. The Mission results provided data on a wide range of planet and planetary systems orbiting both single and multiple stars of differing sizes, temperatures, and ages. The evolution of the *Kepler* Mission started in 1983 (Borucki, 2016) and was based on the then-current assumptions about the frequency and structure of planetary systems (i.e., most stars would have a planetary system, and its structure would be similar to our own).

Prior to the observations of exoplanet systems orbiting neutron stars (Wolszcan and Frail, 1992) and normal stars (Mayor and Queloz, 1995), a simple paradigm (Cameron, 1962) was often invoked to explain the evolution and structure of our Solar System. According to this paradigm, other planetary systems would be similar to the Solar System in having small rocky planets in inner orbits and large ice- and gas-giant planets at distances of several astronomical units (AU). This paradigm assumed that each planetary system would form from a co-rotating disc of gas and dust that resulted from a collapsing portion of a giant molecular cloud. Rocky planets were expected to occur only near the star because the temperature was too high for non-refractory materials to condense. At farther distances, the temperatures were cool enough to condense volatile materials. Embryonic planets in large orbits would quickly sweep up enough material to become so massive that the hydrogen and helium

in the protoplanetary disk would be accreted, thereby producing ice- and gas-giant planets. Because the star and planets formed from the same protoplanetary disk, the planets would lie in a plane that included the stellar equator, and all of the orbits would be prograde (i.e., moving in the same direction as the rotation of the star they orbit). Planets would be found at the location of their formation. Multi-planet systems should be common because they are part of the process of forming stars. Although some of the assumptions in this paradigm are consistent with recent observations, revision and extension of this paradigm are active areas of research (Goldreich, Lithwick, and Sari, 2004; Mordasini, Alibert, and Benz, 2009; Ida and Lin, 2010). The surprises are inspiring new ideas about the processes that control the formation and structure of planetary systems—including our own.

The purpose of this paper is to present some of the science results of the *Kepler* Mission and compare them with what was expected based on the simple paradigm. Descriptions of the instrument and mission design as well as a discussion of the data and their validation are provided in Sections 1 and 2. Section 3 presents the mission results and compares them with the expectations from the paradigm. Section 4 is a summary.

## 1. Instrument and Mission Design

To detect and characterize exoplanets, a space-borne photometer was developed that could continuously measure the brightness of individual stars with the photometric precision necessary to detect Earth-size planets transiting solar-like stars. The photometer searched for the dimming that occurs when an orbiting planet crosses the disk of its star (i.e., "transits" as seen by an observer). Because Earth-size planets are so small compared to their star, the dimming is less than 100 parts per million (ppm) for solar-like stars. Operation in space was necessary to avoid the loss of photometric precision due to the variable transmission through the Earth's atmosphere and the loss of transits due to the day/night cycle and weather. Only those planets that have their orbital plane aligned along the line of sight from the observer to the star can show transits. The geometrical probability of such an alignment for a planet in a particular orbit around a star is the diameter of the star divided by the diameter of the planetary orbit (Borucki and Summers, 1984). That probability is about 10% for very close planets and about 0.5% for planets in the HZ of sun-like stars. To get a statistically significant number of planets from which to derive the frequencies necessary to satisfy mission goals, the Mission simultaneously monitored 170,000 stars. An additional 25,000 stellar objects (i.e., stars, star clusters, and galaxies) were monitored at various times for the Guest Observer

Program (Barclay, 2012). A minimum of three transits was required for detection in order to provide a reliable value for the orbital period, reduce false detections, and increase the overall signal-to-noise ratio (SNR) above the detection threshold. The latter is of particular importance for small planets.

The *Kepler* Mission relied on precise differential photometry to detect the slight signal variation due to the transits of small planets (i.e., the 84-ppm variation for an Earth-Sun-equivalent transit). Such precision required superb instrument stability on timescales up to several times the duration of the transits, systematic error removal to much better than 20 ppm, and a pointing precision of 0.01 arc seconds based on half-hour samples.

The flight segment consists of the photometer and supporting spacecraft. Figure 1 is a cutaway diagram of the *Kepler* instrument. Its design is based on a Schmidt optical system with the array of 42 charge-coupled device (CCD) detectors that cover 105 square degrees at the prime focus. In Figure 2, the focal surface with 21 detector modules is shown. Each module contains a pair of CCDs and is covered by a sapphire field-correcting lens to bring the image from a curved focal surface into focus on the flat detectors. The four small fine-guidance sensors that control the pointing are at the four corners of the focal surface. The Schmidt design was chosen to get the very large field of view (FOV) needed to simultaneously monitor 170,000 stars.

Below the sunshade is a 0.95-m, clear-aperture Schmidt corrector that mitigates the spherical aberration associated with the large FOV and fast optical system. A 1.4 m-aperture mirror is located at the lower end of the telescope structure to focus the light onto the detector array that is placed at the prime focus. The detectors are passively cooled by two heat pipes that conduct the heat from the detector array to the thermal radiator on the outside of the instrument. The sunshade and thermal radiator are visible in Figure 1. The temperature of the detectors is kept at –85°C to minimize the effects of dark current and radiation damage. Four fine-guidance sensors are mounted near the corners of the photometer focal surface to ensure stable pointing and for accurate repositioning of the photometer after the monthly rotations of the spacecraft and antenna to download the data.

Because the observatory orbits the Sun rather than the Earth and because it pointed at only one FOV during the length of the mission, it was rotated 90° every quarter of a spacecraft-year to keep the solar arrays pointed at the Sun and the thermal radiator pointed to deep space. To monitor the maximum number of stars, a region rich in stars near the galactic equator at N76.53°, +13.29° was chosen. On March 9, 2009, the *Kepler* flight segment was launched into a heliocentric orbit with a

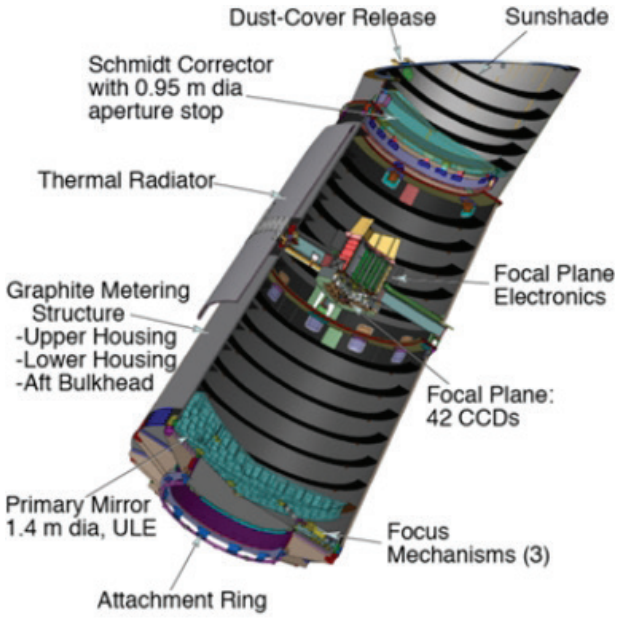


FIGURE 1. Cutaway view of the photometer showing the optics, detector array, detector electronics, thermal radiator, and sunshade. Image courtesy of the Ball Aerospace and Technology Corp (BATC).

period of 372.5 days. Comprehensive descriptions of the mission hardware can be found in Caldwell et al. (2010), Koch et al. (2010), and Borucki (2016).

## 2. Data Description and Validation

Data for all stars were recorded at a cadence of approximately once per 30 minutes, whereas data for a subset of up to 512 stars (chosen each quarter) were recorded at a cadence of approximately once per minute. The shorter-cadence observations were taken to provide high resolution measurements of the ingress and egress times of planetary transits and to conduct the asteroseismic observations needed for measurement of the sizes, masses, and ages of target stars (Chaplin and Miglio, 2013). Stellar characteristics used for the estimation of planet properties were based on Brown et al. (2011) and Huber et al. (2014).

It is important to note that the detection and characterization of exoplanets were based on the brightness variations of individual stars; no spatially resolved images of stars or planets were obtained. "Light curves" represent the time-series data of the brightness variations after the data were calibrated and normalized by various analysis algorithms

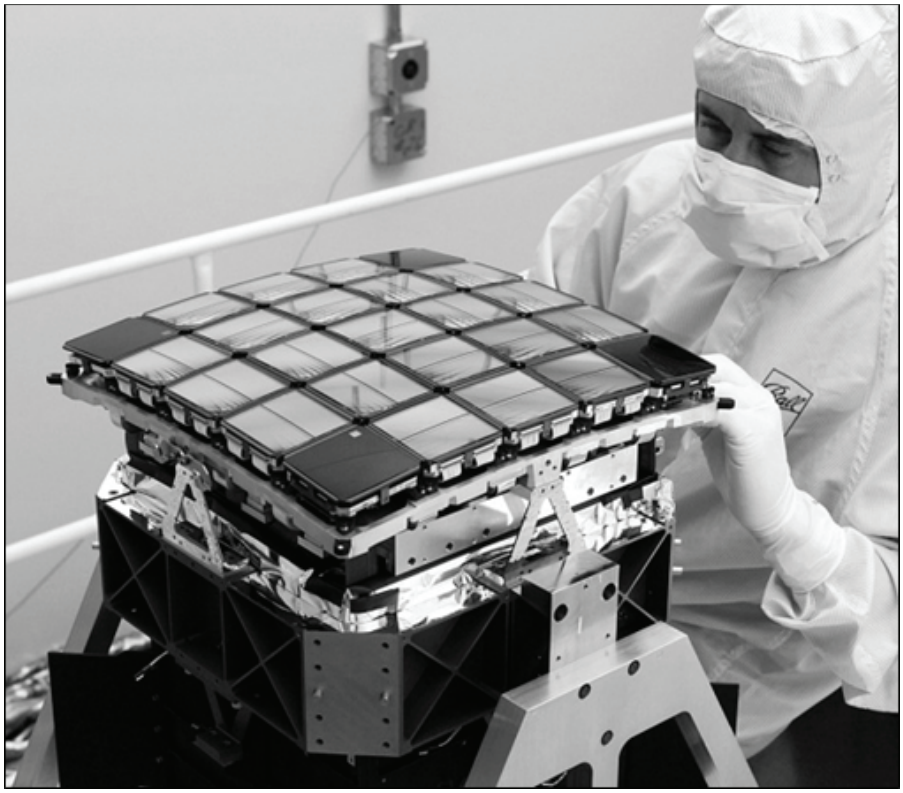

FIGURE 2. Focal surface displaying detector arrays and fine-guidance sensors. The electronics that read out the detectors are directly below the focal surface. Image courtesy of the BATC.

that removed unwanted variations (Jenkins et al., 2010a; Seader et al., 2015). Figure 3 shows an example of a five planet system. The second light curve from the top shows the noisy signature of a small planet with a short-period orbit. The bottom panel shows the much longer transit duration and a deeper minimum that are associated with a large planet in a long-period orbit. The many data points available for planets in short-period orbits compared to the few available for the planet in the longest orbit made it possible to find small planets in inner orbits that might not be detected in long-period orbits. The differing structure and period of transit light curves made identification and characterization of each planet in a planetary system straight forward; the depth of the dips is proportional to the planet size, and the duration of the transit is related to the planet's orbit. Table 1 lists the characteristics of each planet.

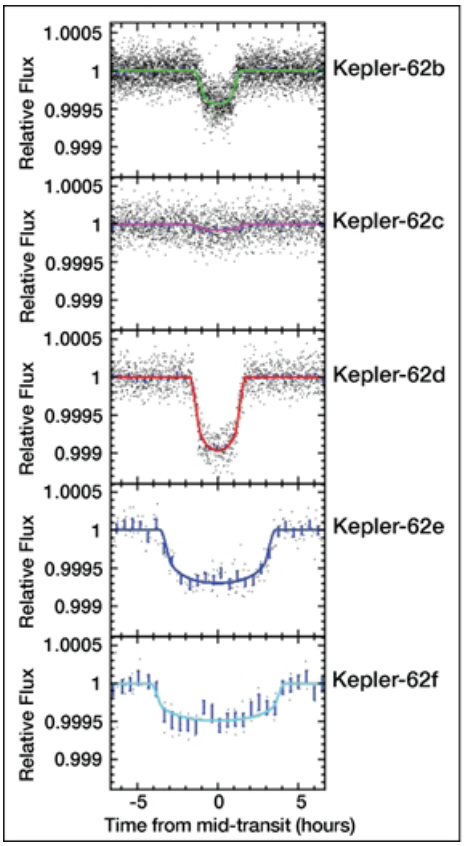


FIGURE 3. Phased light curves for the five planets in the Kepler-62 planetary system (Borucki et al., 2013). Planets 62e and 62f are in the HZ, where liquid water might exist assuming a rocky planet with a suitable atmosphere and albedo (Kopparapu et al., 2013).

In favorable circumstances (i.e., massive planets in short-period orbits around a bright star), ground-based radial velocity (RV) measurements provided the masses of planets discovered by transit photometry (Mayor and Queloz, 1995; Latham et al., 2010; Cochran et al., 2011; Howard et al., 2013; Marcy et al., 2014). Masses of transiting planets were also obtained from the gravitational interaction between planets in nearby orbits because the interactions cause variations in the transit times (Agol et al., 2005; Fabrycky et al., 2012; Ford et al., 2012). The combination of mass and size allows estimates of the planet's density and thereby provides a clue as to whether the planet is a rocky planet like Earth, a gas or ice giant like Neptune and Jupiter, or something quite different.

| Planet | Size ($R_\oplus$) | Depth (ppm) | Period (days) | Duration (hours) |
|---|---|---|---|---|
| 62-b | 1.3 | 430 | 5.7 | 2.3 |
| 62-c | 0.5 | 70 | 12.4 | 3.0* |
| 62-d | 2.0 | 920 | 18.2 | 3.0 |
| 62-e | 1.6 | 700 | 122.4 | 6.9 |
| 62-f | 1.4 | 420 | 267.3 | 7.5 |

*This value has a large uncertainty.

TABLE 1. Planetary characteristics for the Kepler-62 planetary system (Borucki et al., 2013)

*False-positive and False-alarm Events*

There are several astrophysical processes that can mimic planetary transits (Brown, 2003). Common examples include eclipsing binary (EB) stars, in which a smaller star transits a much larger star, and the situation in which the light from a nearby EB is mixed with that of the target star. Thus, the detection of a transit-like pattern from a target star is not sufficient evidence to confirm the presence of a planet orbiting the star. "Candidate" planets are those deduced from an analysis of *Kepler* data but have not yet been independently validated as a "confirmed" planet. Although detailed examination of the *Kepler* data helped to separate image artifacts associated with the data processing (labeled as "false alarms") from real astrophysical events that mimic planetary transits (labeled "false positives"), more data and comprehensive analysis were often necessary to distinguish actual planets from their mimics.

*Follow-up Observations*

Once false alarms were ruled out, follow-up observations were made with large ground-based and space-based telescopes to (a) better characterize the star and thereby obtain accurate estimates of planet size, (b) determine whether the planets were in the HZ, and (c) recognize the false positives. Spectroscopy was used to both characterize the size of the star and search for stellar companions. Images with high spatial resolution, including adaptive optics (AO) and speckle techniques (Howell et al., 2011), were taken to find companion stars that could dilute the signal and identify the star that was the actual source of the signal. Hubble Space Telescope observations to search for close-by companions were made when necessary for high-priority targets. When feasible, infrared observations were made with the Spitzer telescope to test whether the transit amplitude was independent of wavelength, as it

must be if the source of the signal is the target star rather than a nearby faint (red) companion star or a distant (reddened) optical double.

For some candidates, follow-up observations were not feasible, and statistical studies based on comprehensive examinations of the *Kepler* data were not sufficient to exclude all possible events that could mimic planetary transits. These candidates await further investigations before they can be confirmed as planets. Currently, *Kepler* has discovered more than 4,696 planetary candidates and confirmed more than 2,329 as planets.[1]

It is important to note that the *Kepler* observations represent samples taken from parent distributions and that there are many sources of biases that must be considered before an accurate estimate of the parent distributions can be obtained. Pertinent examples of biases follow:

1. The probability of orbital alignment with the line of sight increases with stellar diameter and decreases with semi-major axis, and hence period.
2. Planets in long-period orbits show fewer transits than those in short-period orbits. This bias is especially important for small planets that often have low SNR.
3. Planets orbiting small stars and/or quiet stars are easier to detect than those orbiting large/and or noisy stars because of the higher SNR.
4. Dilution of the signal from a planet orbiting a target star that is near a bright background star reduces the probability of detection of planets orbiting faint stars.
5. Planets orbiting exterior to binary stars are difficult to recognize because of their irregular transit patterns and because of dilution of the light flux by the companion star.

Until the effects of these biases are accurately determined and the full range of orbital periods are considered, estimations of parent distributions come with large uncertainties. In particular, the estimates of the frequency of Earth-size planets in the HZ of solar-like stars (i.e., $\eta_{\oplus}$) are poorly constrained. At present, no exact Earth-analogs (an Earth-size planet orbiting in the HZ of a Sun-like star) have been discovered or confirmed. Thus, current values for $\eta_{\oplus}$ in the literature are extrapolations based on preliminary efforts to correct at least some of the biases but often do not include planets over the full range of orbital sizes (Petigura, Howard, and Mary, 2013; Burke et al., 2015). For planets orbiting GK-type dwarfs with orbital periods near one year, and for planet size of 1 $R_{\oplus}$ ± 20%, Burke et al. (2015) find $\eta_{\oplus}$ to be 0.1 with a

1 NASA Exoplanet Archive, accessed August 2, 2016, http://exoplanetarchive.ipac.caltech.edu

range from $0.01 \leq \eta_{\oplus} \leq 2$. When the range of acceptable planet sizes and orbital periods are increased to $0.75\ R_{\oplus} \leq Rp < 2.5\ R_{\oplus}$, and 50 days $\leq P_{orbit} \leq 300$ days, $\eta_{\oplus}$ increases to 0.77 (Burke et al., 2015).

## 3. Comparison of Mission Results with Expectations

Prior to the availability of the *Kepler* results, most exoplanet detections were largely of planets the size of Jupiter and larger (Mayor et al., 2004: Udry and Santos, 2007). The large range of densities (i.e., from 0.05 gr/cm$^3$ for Kepler-51d to 13 gr/cm$^3$ for Kepler-39b) for giant planets (Southworth, 2012; Masuda, 2014; Borucki, 2016) was unexpected and suggests the complexity of planetary structures. However, the results show that most planets are, in fact, much smaller than Jupiter and most are even smaller than Neptune (Figure 4). The highest frequency of discovered planets is for planet sizes between that of the Earth and Neptune (i.e., for sizes not found in the Solar System). These might represent super-Earths (i.e., rocky planets substantially larger than Earth) or "mini-Neptunes." Planets larger than 1.6 $R_{\oplus}$ are likely to be massive enough to attract a hydrogen-helium atmosphere (Lopez and Fortney, 2014; Marcy et al., 2014; Rogers, 2015), whereas mini-Neptunes are as puzzling as Neptune itself with respect to their structure. It has been suggested (Valencia, O'Connel, and Sasselov, 2006; Sotin, Grasset, and Mocquet, 2007) that some super-Earths might be water planets, or planets with an ice or rocky core covered by an ocean.

Another surprise is the large number of planets found in short-period orbits (Boss, 2000). Whether large or small, most of the planets shown in Figure 4 have orbital periods much shorter than that of Mercury (i.e., 88 days). Although small rocky planets were expected in short-period orbits, the simple planetary-formation paradigm presented in the Introduction implied that giant planets would be found only well beyond Earth's orbit (i.e., with periods of years rather than days).

The recent discovery of a super-Neptune-size planet orbiting close to a 5- to 10-million-year-old star (David et al., 2016) implies that the formation of a giant planet near the host star is possible or that the planet quickly migrated to its current position. Giant planet migration occurs only during the short time while the protoplanetary disk of dust and gas is still present (Goldreich and Tremaine, 1980; Ida and Lin, 2010; Ida, Lin, and Nagasawa, 2013), but that period is consistent with the age of the star (Mordasini, Alibert, and Benz, 2009).

Further examination of Figure 4 shows a gap in detections for planets larger than Earth that have periods less than 10 days. This gap might be caused by high levels of irradiance or the strong stellar winds and ultraviolet activity associated with young stars that removes planetary

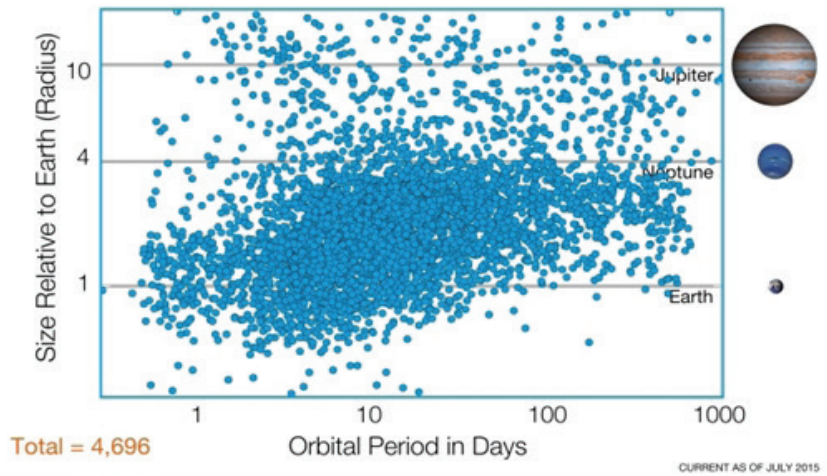


FIGURE 4. *Kepler* observations of exoplanet candidates and confirmed planets (NASA image).

atmospheres and reduces planet size, as well as by the rapid migration of giant planets that brings them to the vicinity of the star prior to the star's entry onto the main sequence. Arrival of a Neptune-size planet during this early phase of stellar evolution (or during the evolution of their atmospheres) could cause much of the atmosphere to be stripped away until only a small, super-Earth-size core remains (Rogers, 2015; Lundkvist et al., 2016). Gas giants that arrive after the period of extreme stellar activity or with a massive core that prevents atmospheric stripping might explain the data points seen in the top-left of Figure 4.

Figure 4 represents the sample distribution rather than the parent distribution. Because it is much easier to find large planets than small ones, it is likely that planets smaller than Neptune are even more plentiful than shown here. After correcting for this bias and several others, calculations Burke et al., 2015 indicate that the frequency of planets rises abruptly as the planet size decreases below that of Neptune. The results shown in Figure 5 are based on the analysis of nearly four years of *Kepler* data for G- and K-type stars (Burke et al., 2015). Although their results are only preliminary (because they do not yet include all systematic errors and include only orbital periods between 10 and 300 days), their results indicate that the number of planets per star is of order 1 (i.e., planets are as plentiful as stars in our galaxy).

Giant planets orbiting close to bright stars sometimes reflect and emit sufficient light that the occultations as well as the transits can be recognized (Figures 6a and 6b). The folded light curve based on *Kepler* observations (Borucki et al., 2009) of HAT-P-7b (Pál et al., 2008) is shown in Figure 6a. The two large-amplitude dips are the transits of a

Jupiter-size planet in a 2.2-day orbit, whereas the slight depression between the two transits is due to the occultation as the planet moves behind the star. In the top panel of Figure 6b, the vertical scale is expanded, and the horizontal scale is restricted to just the interval centered on the occultation. The amplitude of the light curve is a maximum near the occultation. This variation is caused by the combination of the increase of the reflected light from the planet as it moves from inferior conjunction to superior conjunction, the ellipsoidal variation of the star due to tides raised by the nearby massive planet, and by Doppler boosting (Welsh et al., 2010). Doppler boosting is the change in the stellar flux as the star moves toward and away from the observer, combined with the stellar color change convolved with the wavelength response of the *Kepler* photometer.

In the second panel from the top in Figure 6b, the model (Angerhausen, DeLarme, and Morse, 2015) of the sum of these processes is shown in black. The best fit to the reflected light from the planet is shown in red. However, the light fluxes from both Doppler-boosting (green) and the tidal distortion of the star (blue) add to the reflected light to give a more complex light curve than that of the reflected light alone.

The bottom two panels of Figure 6b show similar results for exoplanet Kepler-13b. Here, the effect of the ellipsoidal change in the star shape is large enough to overwhelm the phase curve due to the changing illumination of the planet. Consequently, the light curve slopes downward near the occultation. The asymmetry in the measured curve is associated with the Doppler-boosting and the fact that the planetary orbit is eccentric, whereas the model assumes a circular orbit (Angerhausen, DeLarme, and Morse, 2015).

Radiation emitted from a hot planet can also be important (Placek, Knuth, and Angerhausen, 2014). Examination and modelling of the light curve allow the planet albedo and temperature to be determined. The amplitude of the Doppler-boosting is sometimes so sufficiently large that the mass of the planet-to-star mass ratio can be determined (Esteves, De Mooij, and Jayawardhana 2015). This method of estimating planet mass is an important addition to the RV and transit-timing methods. It is especially useful for hot stars because they generally do not show sufficiently detailed spectra to allow mass determinations from spectroscopic (i.e., RV) measurements.

One of the biggest surprises from the *Kepler* Mission was the discovery of many "super-Earths," or planets bigger than Earth but smaller than Neptune. Because the Solar System has no super-Earths and because most of the discovered super-Earths have no measurements of mass or density, their composition and structure are uncertain. The planets could have a rocky-composition like Earth, or they

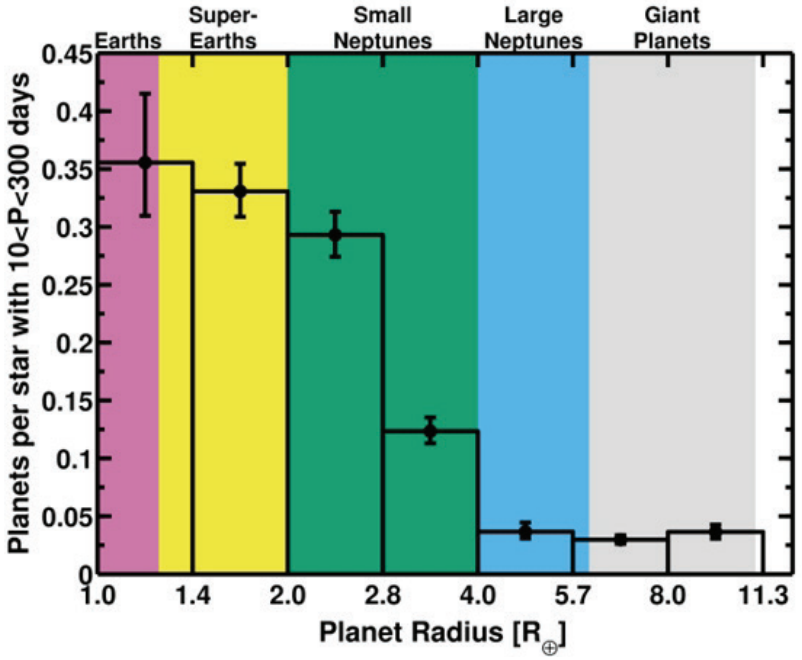


FIGURE 5. Estimate of the size distribution of *Kepler* exoplanet candidates and confirmed planets orbiting G- and K-type stars with periods between 10 and 300 days after corrections for survey biases. Error bars include only the statistical uncertainty with the number of events. Personal communication from Burke (2016), based on the calculations of Burke et al., 2015.

might be gas and ice giants like Neptune and Uranus. However, model calculations suggest the possibility that the super-Earths could be unlike either and instead be composed of water and ice with a smaller amount of rocky material (Kuchner, 2003; Leger, et al., 2004). The planets might have a highly-compressed thick layer of ice with an overlying ocean and a water-vapor atmosphere (Valencia, O'Connel, and Sasselov, 2006; Sotin, Grasset and Mocquet, 2007). Figure 7 is an artist's sketch of *Kepler's* first super-Earth planet (Borucki et al., 2012) found in the HZ. The size of Kepler-22b (2.4 $R_{\oplus}$) places it in the middle to the range between that of Earth and Neptune (1.0 and 3.8 $R_{\oplus}$, respectively). It has an orbital period of 289.9 days slightly shorter than the Earth's orbit and orbits a star slightly cooler than the Sun (5518K vs. 5780K, respectively). Calculations (Neubauer et al., 2012) indicate that Kepler-22b is in the HZ, regardless of whether the solvents are water, ammonia/water, or sulfuric acid.

Combined with nitrogen and carbon dioxide (both commonly found in the solar system), the water evaporated from the ocean could form an

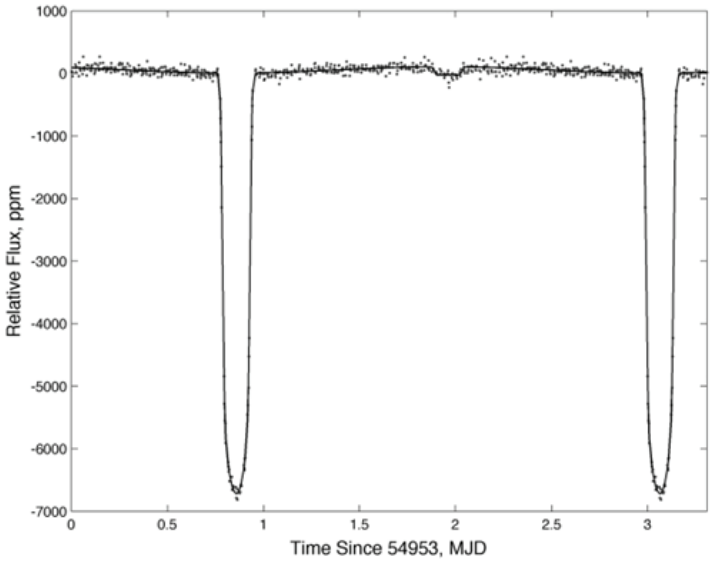


FIGURE 6a. Kepler observations of HAT-P7b showing two transits and an occultation midway between the transits (Borucki et al., 2009).

atmosphere conducive to life. Stellar UV radiation would photodissociate the water to form an ozone layer. A determination of whether planets like Kepler-22b actually have oceans, atmospheres conducive to life, and life must await the results of more capable missions.

It might be expected that orbital planes would be aligned with the equatorial plane of a star because the star was formed from the same disk of gas and dust that formed the star and its planets. However, the numerical model of Jurić and Tremaine (2008) for the formation of planetary systems predicts that gravitational interactions among giant planets will result in more than 10% having inclinations $\geq 25°$ between that of the planetary orbit and the star's equator. Recent observations (Xue and Suto, 2016) show the fraction is approximately 25%.

A distinct contribution of the *Kepler* measurements to the structure and characteristics of a planetary system is presented in Huber et al. (2013). The *Kepler* observations of the stellar power spectra of Kepler-56 show sets of gravity- and pressure-dominated modes that indicate the spin axis of the red giant is tilted at about 47° to the line of sight and to the planetary orbital planes of Kepler-56b and Kepler-56c. Analysis of the asteroseismology results provide accurate size determinations for the star and planets; $4.23 \pm 0.15\ R_{\oplus}$, $6.51 \pm 0.29\ R_{\oplus}$, and $9.80 \pm 0.46\ R_{\oplus}$, respectively. Transit timing variations of the planets (Figure 8) combined with additional RV measurements provide estimates of the masses and densities for both planets and are consistent

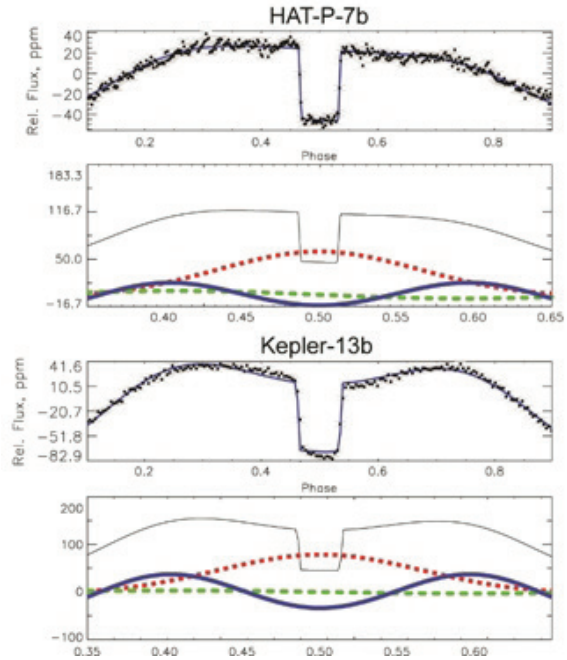


Figure 6b. Phase curves showing light variations due to reflected light from the planet and variations in stellar ellipticity and Doppler boosting (modified from Angerhausen, DeLarme, and Morse, 2015, with permission). The top panel expands the vertical scale of the observations shown in Figure 6a. The second panel shows the components of the model. The light black line represents the sum of the components, the red dashed line represents the reflected light from the planet, the solid blue line represents the ellipsoidal variation of star, and the dashed green line represents the effect of Doppler-boosting and the effects of the spectral shift convolved with the wavelength dependence of the instrument response function. The two lower panels compare the measurements and observations and display the model components for Kepler-13b.

with circular coplanar orbits. The RV observations also detected a long-period object that could account for the stellar obliquity.

A possible explanation for the non-zero obliquity is that two planets gravitationally interacted through Kozai-Lidov resonance mechanism during the evolution of the planetary system (Rasio and Ford, 1996; Fabrycky and Tremaine, 2007; Petrovich, 2015). In this scenario, gravitational interaction between the outer and inner companions cause the inner planet to move into a highly elliptical orbit while simultaneously changing its obliquity. The orbit of a massive planet in a highly eccentric orbit can be circularized by tidal interactions with the star when the planet is near periapsis (Ivanov and Papaloizou, 2007).

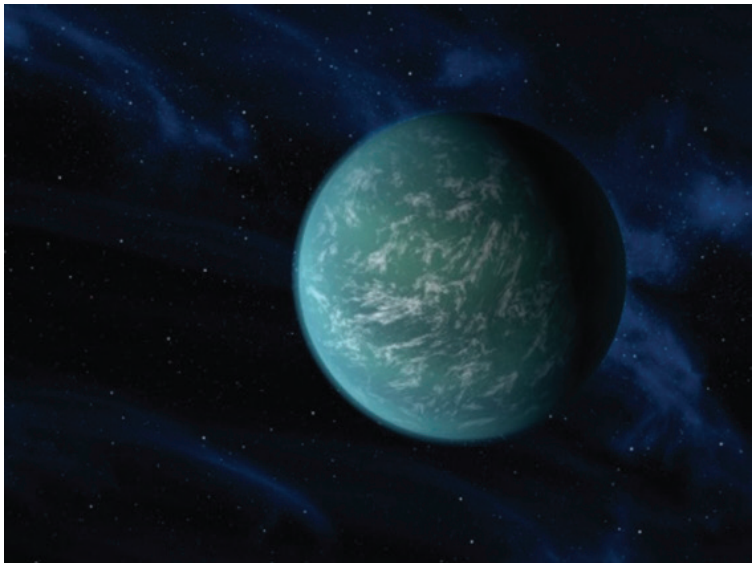

FIGURE 7. Artist's conception of Kepler-22b, a possible ocean planet that was confirmed in the HZ (NASA image).

Based on the simple paradigm of planetary system formation, it is expected that planets and planetary systems should be found around most stars. This prediction has proven to be consistent with observations; most stars have planets, and multi-planet systems are common (Figure 9). Batalha (2014) finds that the frequency of stars found with multi-planet systems is 22%, whereas Rowe et al. (2014) find the frequency of candidates that are part of multi-planet systems is 40%. It should be noted that multi-planet systems with a diversity of orbital inclinations could appear to be a single-planet system. Thus, the fraction of multi-planet system is likely to be higher than implied by transit observations.

Although the high frequency of planetary systems was expected, their varied structure was not expected. As discussed earlier, the paradigm of planetary system evolution predicts that planetary systems would be similar to the Solar System in having small rocky planets occupying inner orbits and larger gas and ice giants occupying outer orbits. However, the *Kepler* discoveries show that the orbital positions of exoplanets appear to be nearly random regardless of their size (Figure 9). As Mayor and Queloz (2012) state: "The solar system does not appear as a typical example of planetary systems."

The somewhat higher frequency of small planets with short-orbital periods shown in Figure 9 could be due to the difficulty of their detection at longer periods with fewer transits. Several theories have been developed to explain the observations. One theory (Ida and Lin, 2010; Ida, Lin, and

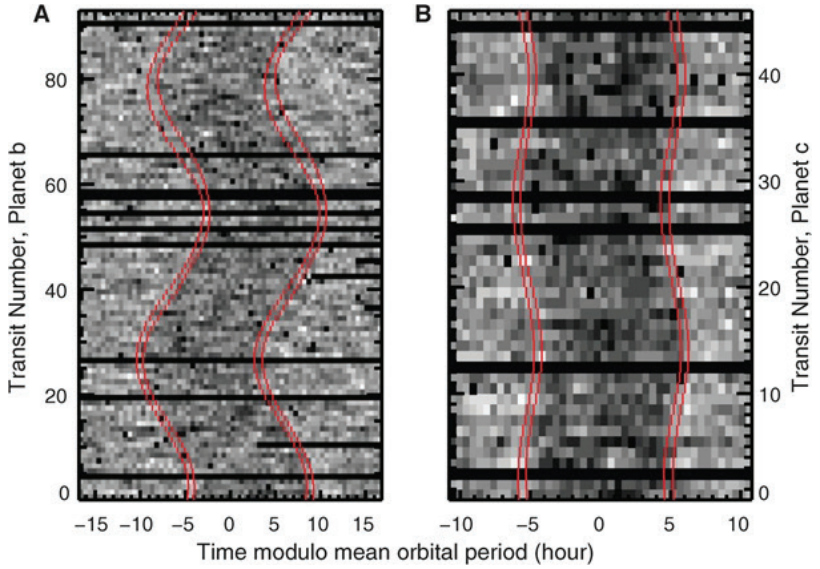


FIGURE 8. Transit time variations of the inner planets of Kepler-56. Stellar intensity is plotted as a function of the transit epoch and the modulo of the mean orbital period near transits of Planet b (left panel) and Planet c (right panel). The red lines mark the 68% confidence intervals for the start and end of each transit according to the model calculations (Huber et al., 2013, with permission) The anticorrelation in time indicates that both planets orbit the same star and allows estimates of their masses.

Nagasawa, 2013) notes that an embryonic planet will be traveling faster than the gas and dust in the protoplanetary disk, which will cause the formation of dissipative waves that will remove the planet's momentum and cause it to migrate inward. Calculations (Goldreich and Tremaine, 1980) show the situation to be more complex in that various density distributions of the protoplanetary disk can cause migration both inward and outward from the star. Even the gravitational interaction due to the presence of nearby planets can cause migration through the development of Kozai resonances as discussed earlier.

Planetary systems that are much more compact than the Solar System were not predicted yet appear to be common. Figure 10 compares semi-major axis values for planets in five compact systems with all or most of the planets with orbits shorter than that of Mercury. Many of these planets are within 0.1 AU of the host stars, and two are within 0.02 AU. It was believed that the interaction of closely spaced planets would cause instabilities that would rule out their occurrence or at least make them rare. The processes that lead to their tight packing, stability, and the narrow range of the planetary obliquities are active areas of investigation.

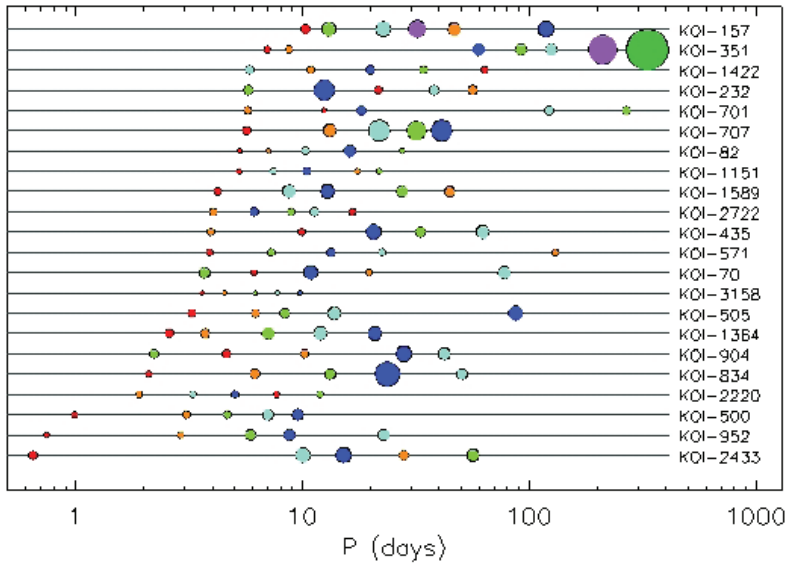


FIGURE 9. Structures of several multi-planet systems discovered by the *Kepler* Mission (Fabrycky, personal communication, 2014).

The Kepler-444 system shown in Figure 10 is a particularly interesting compact system. It is an example of a system 6 billion years older than the Solar System, as determined from asteroseismology results (Campante et al., 2015). The fact that the planets are so small and close to the host star implies that they are likely to be rocky planets. Its age shows that planetary systems were being formed from the start of the evolution of our galaxy. Because the formation of planetary systems containing rocky planets started so early in the history of our galaxy, many such planets must be billions of years older than Earth. If life exists on these planets, the products of evolution are likely to be beyond our imagining.

About one half of the solar-type stars in our galaxy are known to be part of multi-star systems—mostly binary systems (Raghavan et al., 2010). The many processes involved in the formation and evolution of planetary systems are so complex that models have not yet provided estimates for the relative frequency and structures of planetary systems orbiting single and multiple stars. Recent data should provide some guidance for the development of such theories. Currently, *Kepler* has found 11 circumbinary systems. All of these orbit beyond the critical distance for instability (Holman and Wiegert, 1999). Planets orbiting each star of a binary pair have also been found (e.g., Kepler-132ABbcd [Lissauer et al., 2014]), as well as a planet orbiting a binary star in a four-star system (Schwamb et al., 2013).

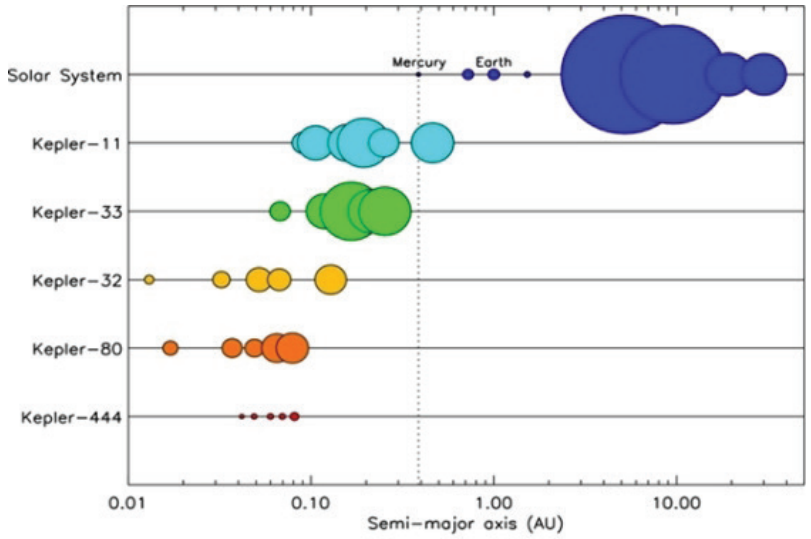


FIGURE 10. Comparison of the Solar System with examples of very compact systems. The symbol size is proportional to planet diameter. The horizontal scale for the semi-major axis is logarithmic (Campante et al., 2015).

Figure 11 is an artist's depiction of the Kepler-47 planetary system that has two planets orbiting a pair of dwarf stars. The brighter of the two stars has a temperature and size similar to the Sun (5636K and 1.04 $R_{\oplus}$). The outermost planet, Kepler-47c, is in the HZ and has an orbital period of 303.2 days. It receives an average heat and light flux similar to that received by the Earth (i.e., 0.87 $S_{0)}$. For comparison, Mars and Venus receive 0.43 and 1.91 $S_0$, respectively. Because Kepler-47c is much larger than Neptune (4.6 $R_{\oplus}$), it is likely to have an extended hydrogen/helium atmosphere and to be an ice-giant without a rocky surface. However, moons orbiting planets in the HZ would also be in the HZ. If such moons contained a massive atmosphere like that on Titan, it is conceivable that life might evolve on them. Kipping et al. (2013) describe an early (unsuccessful) search for moons orbiting *Kepler* planets.

The complexity of the transits, eclipses, and occultations of even a single planet in a binary star system makes it difficult to recognize the transit signatures (Welsh et al., 2012). An example of the complexity is illustrated in Figure 12 (Doyle et al., 2011). Light curves for multiple planets orbiting in many-star systems are even more complex because of the multiplicity of planets, noise, and in some cases, the precession of the orbital planes (Carter et al., 2011) that cause alternating periods when transits are present and when they are absent.

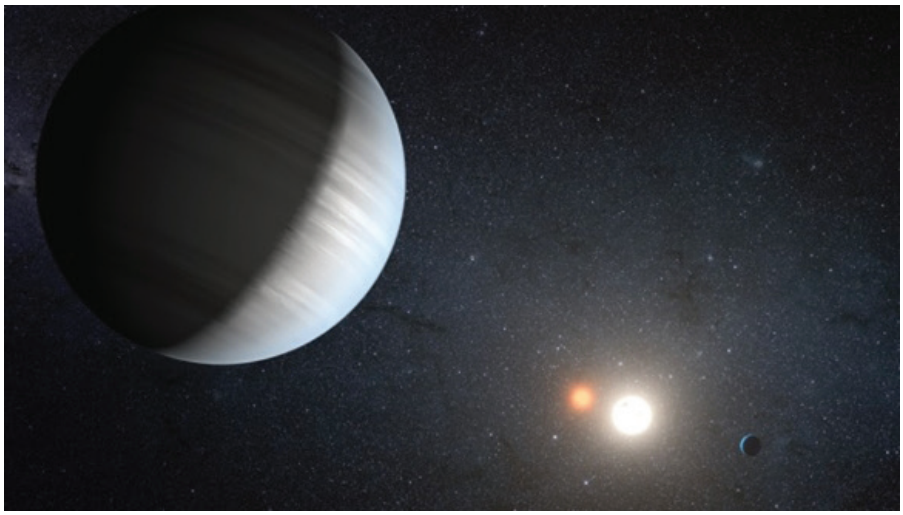

FIGURE 11. Artist's depiction of Kepler-47. A planetary system orbiting a double star with one of the two planets in the HZ (Orosz et al., 2012).

More than one-dozen Earth- and super-Earth-size planets have been discovered in the HZ (Burke et al., 2015). Figure 13 presents both current candidates and confirmed planets in the HZ. A comprehensive analysis by the Kepler Team to correct for all known biases and to provide reliable estimates of the frequency of Earth- and super-Earth-size planets in the HZ is underway.

The large sample of consistently observed data for many stars enabled techniques that used the stacking of *Kepler* data of multiple exoplanetary systems to search for effects that were too subtle to be detected in single systems. Sheets and Deming (2014) found secondary eclipses of super-Earths, Hippke (2015) found evidence for moons, and Hippke and Angerhausen (2015) found signatures of an exoplanetary Trojan asteroid population using methods that combined and phase-folded data from many *Kepler* objects to reach sensitivities of a few ppm.

One of the most mysterious of all the *Kepler* detections is shown in Figure 14. The light curves shown represent nearly four years of *Kepler* observations of a 12th-magnitude, F3 spectral-type, main-sequence star KIC8462852. The puzzling pattern of deep and complex-shaped transits is unlike those due to planetary transits or eclipsing multiple-star systems. The pattern has generated much speculation about its source. Transit depths of 15% and 20% seen near days 793 and 1,520 indicate an object that is nearly one-half the size of the host star. Boyajian et al. (2016) suggest a group of comets as the source but note that the depth is so great that the explanation is difficult to defend. A model calculation by Bodman and Quillen (2016) show that a dense swarm of comets might

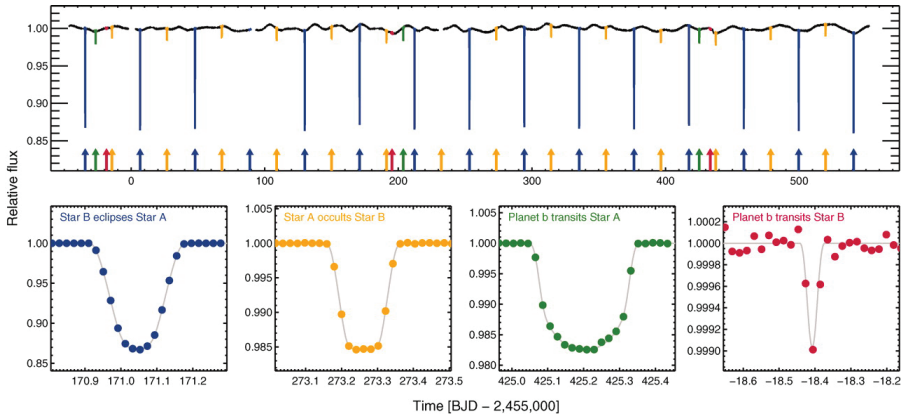


FIGURE 12. Light curves for Kepler-16b showing complexity of transit signatures for a single planet orbiting a binary star. Blue arrows point to the occultation when Star B is eclipsing Star A; yellow arrows point to the occultations of Star A by Star B; green arrows point to the transits of Planet b across Star A; and red arrows point to the transit of Planet b across Star B (Doyle et al., 2011).

fit the later data. If the comets are about 100 km in size, then they can also fit the early transit event. However, Wright et al. (2016) speculate that the source could also be explained as artificial structures made by an advanced civilization. Although *Kepler* spacecraft can no longer monitor this object, the signal amplitudes are so large that ground-based instruments have the necessary precision to make the follow-up observations needed to provide further information.

## 4. SUMMARY

During the four years of operation, *Kepler* made an unprecedented set of time-series observations of 195,000 stars and discovered 4,696 planetary candidates that range in size from slightly larger than the Moon to planets more than three times larger than Jupiter.

Many of the results differed from what was expected based on the simple planetary system formation paradigm used to design the Mission. These results include:

1. Planetary system architectures are unlike that of the Solar System.
2. Giant planets are often found closer to their host star than Mercury is to the Sun.
3. Very compact planetary systems with non-rocky planets orbiting very close to their host star are frequent.

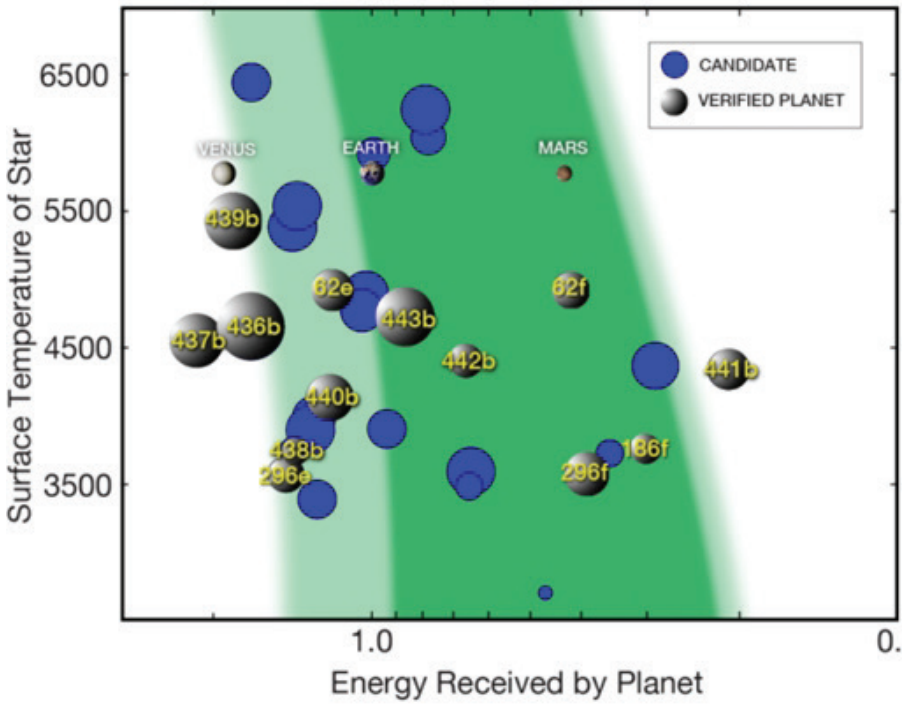


FIGURE 13. Earth- and super-Earth-size planets and planetary candidates in the HZ. Stellar insolation at the semi-major axis of the planet versus stellar effective temperature. The dark green area is the conservative estimate, whereas the light green shows the limits for the "optimistic" zone (Kopparapu et al., 2013). Yellow numbers refer to verified planets. Blue circles refer to unconfirmed planetary candidates. The sizes of the circles are scaled to that of the Earth. The curvature shown for the HZ bands is caused by a slight dependence of the flux at the surface of the planet on the stellar temperature (Borucki, 2016).

4. Most of the discovered planets are sizes between that of rocky planets like the Earth and gas and ice giants like Neptune and Jupiter (i.e., they are unlike any of the planets in the Solar System). Model studies indicate that some of these intermediate-size planets could be composed of water or ocean-covered.
5. The characteristics of many exoplanets are also unlike those found in the Solar System; some of these are much larger than Jupiter, and some have extremely low densities.

A number of expectations have been confirmed:

1. Most stars have planets.
2. Earth-size planets are common.
3. Planets are found orbiting all types of stars.
4. Planets are found orbiting multiple-star systems.

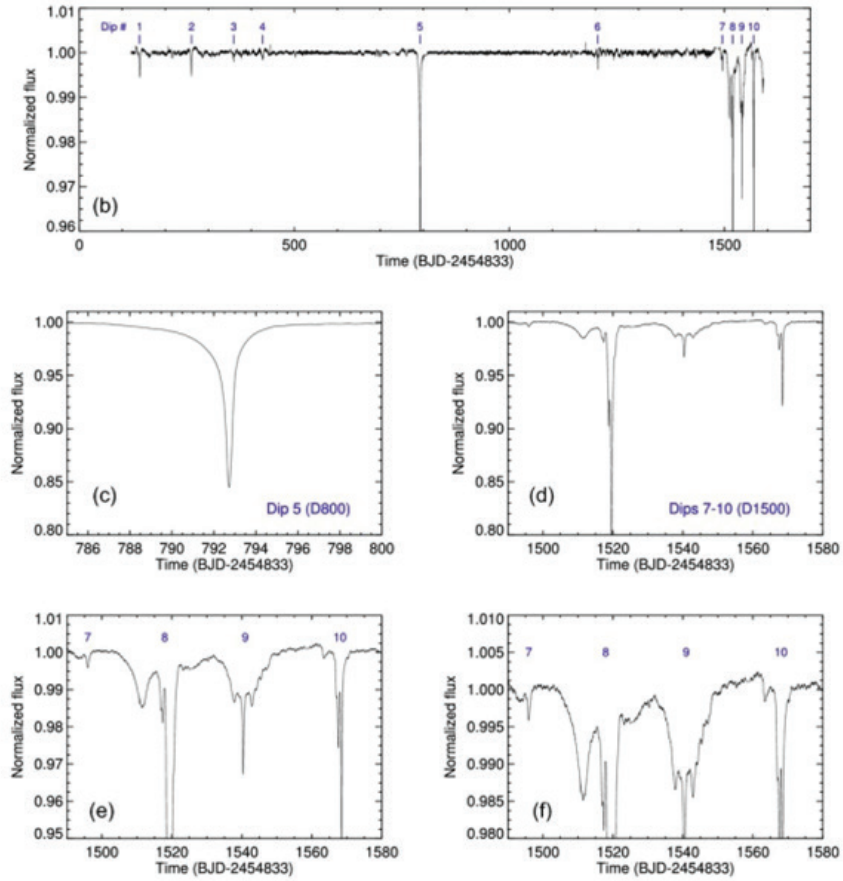


FIGURE 14. *Kepler* light curves of a mysterious event. The bottom two panels are magnifications of the events in the top panel (Boyajian et al., 2016, with permission).

The plethora of new data for planetary characteristics and planetary-systems structures is inspiring further development of theories of planetary formation and evolution. By proving that high precision photometry was practical, the *Kepler* Mission has inspired the development of several new missions (Howell et al., 2014; Rauer et al., 2014; Ricker et al., 2014) that will provide a more comprehensive picture of exoplanet systems. Ultimately, interactions between the new discoveries and the evolving theories of planetary system formation will better define the evolution of the Solar System. *Kepler* has truly been a NASA Discovery-class Mission.

*Acknowledgments*

The author would like to especially thank Daniel Angerhausen, Tiago

Campante, and Daniel Fabrycky for their valuable comments and review of the paper.

*Kepler* was a PI-led, competitively selected mission, the tenth in the NASA Discovery-Program. Funding for this mission is provided by NASA's Science Mission Directorate. Some of the data presented herein were obtained at the W. M. Keck Observatory, which is operated as a scientific partnership among the California Institute of Technology, the University of California, and the National Aeronautics and Space Administration. The Keck Observatory was made possible by the generous financial support of the W. M. Keck Foundation. The author wishes to recognize the significant cultural role of the summit of Mauna Kea to the indigenous Hawaiian community and to thank them for the opportunity to share it in the pursuit of knowledge. The author also wishes to acknowledge that the Mission's success was the result of the *Kepler* team; scientists throughout the world; NASA managers at Ames, JPL, Headquarters, and the Ball Aerospace and Technology Corporation that designed and built the *Kepler* spacecraft; the Laboratory for Atmospheric and Space Physics that controls and commands the spacecraft; and the Mikulski Archive that stores the data and provides them to the public.

## References

Agol, E., et al., "On Detecting Terrestrial Planets with Timing of Giant Planet Transits," *MNRAS* **359 (2005):** 567–79.

Angerhausen, D., DeLarme, E., and Morse, J. A., "A Comprehensive Study of *Kepler* Phase Curves and Secondary Eclipses: Temperatures and Albedos of Confirmed *Kepler* Giant Planets," *PASP* 127 (2015): 1113–30.

Barclay T., "The Kepler Guest Observer Programme, New Horizons in Time-Domain Astronomy," *Proc. IAU Symp.* #285, IAU (2012), doi:10.1017/S1743921312000798

Batalha, N. M., "Exploring Exoplanet Populations with NASA's *Kepler* Mission," *PNAS* 111 (2015): 12647–54.

Bodman, E. H. L., and Quillen, A., "KIC 8462852: Transit of a Large Comet Family," *ApJL* 819 (2016): L34.

Borucki, W. J., "*Kepler* Mission: Development and Overview," *Reports on Prog. in Physics* 79 (2016), doi 10.1088/0034-4885/79/3/036901

Borucki, W. J., and Summers, A. L., "The photometric method of detecting other planetary systems," *Icarus* 58 (1984): 121–34.

Borucki, W. J., et al., "*Kepler's* Optical Phase Curve of the Exoplanet HAT-P-7," *Science* 325 (2009): 709.

Borucki, W. J., et al., "Kepler-22b: A 2.4 Earth-radius Planet in the Habitable Zone of a Sun-like Star," *ApJ* 745 (2012): 120.

Borucki, W. J., et al., "Kepler-62: A Five-planet System with Planets of 1.4 and 1.6 Earth Radii in the Habitable Zone," *Science* 340 (2013): 587.

Boss, A. P., "From Disks to Planets: An Overview," in *ASP Conference Serie*s, Vol. 219 (2000), eds. F. Garzón, C. Eiroa, D. de Winter, and T. J. Mahoney.

Boyajian, T. S., et al., "Planet Hunters IX. KIC 8462852: Where's the Flux?" *MNRAS* 457 (2016): 3988–4004.

Brown, T. M., "Expected Detection and False Alarm Rates for Transiting Jovian Planets," *ApJL* 593 (2003): L125–8.

Brown, T. M., et al., "Kepler Input Catalog: Photometric Calibration and Stellar Classification," *Astron. J.* 142 (2011): 112.

Burke, C. J., personal communication, 2016.

Burke, C. J., et al., "Terrestrial Planet Occurrence Rates for the *Kepler* GK Dwarf Sample," *ApJ* 809 (2015): 8B.

Caldwell, D. A., et al., "Instrument Performance in *Kepler's* First Months," *ApJL* 713 (2010): L92.

Cameron, A. G. W., "The Formation of the Sun and Planets," *Icarus* 1 (1962): 13.

Campante, T. L., et al., "An Ancient Extrasolar System with Five Sub-Earth-size Planets," *ApJ* 799 (2015): 170.

Carter, J., et al., "KOI-126: A Triply Eclipsing Hierarchical Triple with Two Low-mass Stars," *Science* 331 (2011): 562C.

Chaplin, W. J., and Miglio, A., "Asteroseismology of Solar-type and Red-giant Stars," *Annu. Rev. Astron. Astrophys.* 51 (2013): 353–92.

Cochran, W. D., et al., "Kepler-18b, c, and d: A System of Three Planet Confirmed by Transit Timing Variations, Lightcurve Validation, Warm-Spitzer Photometry, and Radial Velocity Measurements," *ApJS* 197 (2011): 7.

David, T., et al., "A Neptune-sized Transiting Planet Closely Orbiting a 5–10 Million Year Old Star," *Nature* 534 (2016): 658.

Doyle L. R., et al., "Kepler-16: A Transiting Circumbinary Planet," *Science* 333 (2011): 1602.

Esteves, L. J., De Mooij, J. W., and Jayawardhana, R., "Changing Phases of Alien Worlds: Probing Atmosphere of *Kepler* Planets with High-precision Photometry," *ApJ* 805 (2015): 150.

Fabrycky, D. C., personal communication, 2014.

Fabrycky, D. C., and Tremaine, S., "Shrinking Binary and Planetary Orbits by Kozai Cycles with Tidal Friction," *ApJ* 669 (2007): 1298.

Fabrycky, D. C., et al., "Transit Timing Observations from *Kepler* IV: Confirmation of Four Multiple-planet Systems by Simple Physical Models," *ApJ* 750 (2012): 114F.

Ford, E., et al., "Transit Timing Observations from *Kepler* V: Transit Timing Variations Candidates in the First Sixteen Months from Polynomial Models," *ApJ* 756 (2012): 185.

Goldreich, P., and Tremaine, S., "Disk-satellite interactions," *ApJ* 241 (1980): 425.

Goldreich, P., Lithwick, Y., and Sari, R., "Final Stages of Planet Formation," *ApJ* 614 (2004): 497.

Hippke, M., "On the Detection of Exomoons: A Search in Kepler Data for the Orbital Sampling Effect and the Scatter Peak," *ApJ* 806 (2015): 51.

Hippke, M., and Angerhausen, D., "A Statistical Search for a Population of Exo-Trojans in the Kepler Data Set," *ApJ* 811 (2015): 1.

Holman, M. J., and Wiegert, P. A., "Long-term Stability of Planets in Binary Systems," *ApJ* 117 (1999): 621.

Howard, A., et al., "A Rocky Composition for an Earth-sized Exoplanet," *Nature* 503 (2013): 381.

Howell, S., et al., "Speckle Camera Observations for the NASA *Kepler* Mission Follow-up Program," *AJ* 142 (2011): 19.

Howell, S., et al., "The K2 Mission: Characterization and Early Results," *PASP* 126 (2014): 398–408.

Huber, D., et al., "Stellar Spin-orbit Misalignment in a Multiplanet System," *Science* 342 (2013): 333.

Huber, D., et al., "Revised Stellar Properties of *Kepler* Targets for the Quarter 1-16 Transit Detection Run," *ApJS* 211 (2014): 2.

Ida, S., and Lin, D. N. C., "Toward a Deterministic Model of Planetary Formation VI: Dynamical Interaction and Coagulation of Multiple Rocky Embryos and Super-earth Systems around Solar-type Stars," *Astrophys. J.* 719 (2010): 810–30.

Ida, S, Lin, D. N. C., and Nagasawa, M., "Toward a Deterministic Model of Planetary Formation VII: Eccentricity Distribution of Gas Giants," *Astrophys. J.* **775** (2013): 42 (25pp), doi:10.1088/0004-637X/775/1/42

Ivanov, P. B., and Papaloizou, J. C. B., "Dynamic Tides in Rotating Objects: Orbital Circularization of Extrasolar Planets for Realistic Planet Models," *MNRAS* 376 (2017): 682–704.

Jenkins, J. M., et al., "Overview of the *Kepler* Science Processing Pipeline," A*pJL* 713 (2010a): L87.

Jurić, M., and Tremaine, S., "Dynamical Origin of Extrasolar Planet Eccentricity Distribution," *ApJ* 686 (2008): 603.

Kipping, D. M., et al., "The Hunt for Exomoons with *Kepler* (HEK) III: The First Search for an Exomoon around a Habitable-zone Planet," *ApJ* 777 (2013): 134.

Koch, D. G., et al., "*Kepler* Mission Design, Realized Photometric Performance, and Early Science," *ApJL* 713 (2010): L79.

Kopparapu, R. K., et al., "Habitable Zones around Main-sequence Stars: New Estimates," *ApJ* 765 (2013): 131K.

Kuchner, M. J., "Volatile-rich Earth-mass Planets in the Habitable Zone," *ApJ* 596 (2003): L105–8.

Latham, D., et al., "Kepler-7b: A Transiting Planet with Unusually Low Density," *ApJL* 713 (2010): L140.

Leger, A., et al., "A New Family of Planets? 'Ocean Planets,'" *Icarus* 169 (2004): 499.

Lissauer, J. J., et al., "Validation of *Kepler's* Multiple Planet Candidates II: Refined Statistical Framework and Descriptions of Systems of Special Interest," *ApJ* 784 (2014): 44.

Lopez, E. D., and Fortney, J. J., "Understanding the Mass-radius Relations for Sub-Neptunes: Radius as a Proxy for Composition," *ApJ* 792 (2014): 1.

Lundkvist, M. S., et al., "Hot Super-Earths Stripped by Their Host Stars," *Nature Comm*. 7 (2016): 11201.

Marcy, G. W., et al., "Masses, Radii, and Orbits of Small *Kepler* Planets: The Transition from Gaseous to Rocky Planets," *ApJ*S 210 (2014): 20.

Masuda, K., "Very Low Density Planets around Kepler-51 Revealed with Transit Timing Variations and an Anomaly Similar to a Planet-planet Eclipse Event," *ApJ* 783 (2014): 53.

Mayor, M., and Queloz, D. "First Discovery (RV) of Exoplanet around a Main-sequence Star," *Nature* 378 (1995): 355.

Mayor, M., and Queloz, D., "From 51 Peg to Earth-type planets," *New Astron. Revs*. 56 (2012):19.

Mayor, M., et al., "The CORALIE Survey for Southern Extra-solar Planets XII: Orbital Solutions for 16 Extra-solar Planets Discovered with CORALIE," *AandA* 415 (2004): 391.

Mordasini, C., Alibert, Y., and Benz, W., "Extrasolar Planet Population Synthesis I: Method, Formation Rracks, and Mass-distance Distribution," *AandA* 501 (2009): 1139.

Neubauer, D., et al., "The Life Supporting Zone of Kepler-22b and the *Kepler* Planetary Candidates: KOI268.01, KOI1701.03, KOI854.01, and KOI 126.01," *Plan. and Space Sci.* 73 (2012): 397.

Orosz, J. A., et al., "Kepler-47: A Transiting Circumbinary Multiplanet System," *Science* 337 (2012): 1511–4.

Pál, A., et al., "HAT-P-7b: An Extremely Hot Massive Planet Transiting a Bright Star in the *Kepler* Field," *ApJ* 680 (2008): 1450.

Petigura, E., Howard, A., and Marcy G., "Prevalence of Earth-size Planets Orbiting Sun-like Stars," *PNAS* 110 (2013): 19273.

Petrovich, C., "Steady-state Planet Migration by the Kozai-Lidov Mechanism in Stellar Binaries," *ApJ* 799 (2015): 27.

Placek, B., Knuth K. H., and Angerhausen, D., "EXONEST: Bayesian Model Selection Applied to the Detection and Characterization of Exoplanets via Photometric Variations," *ApJ* 795 (2014): 112.

Raghavan, D., et al., "A Survey of Stellar Families: Multiplicity of Solar-type Stars," *ApJS* 190 (2010): 1.

Rasio, F. A., and Ford, E. B., "Dynamical Instabilities and the Formation of Extrasolar Planetary Systems," *Science* 274 (1996): 954–6.

Rauer, H., et al., "The PLATO 2.0 Mission," *Experimental Astronomy* 38 (2014): 249–330.

Ricker, G. R., et al., "Transiting Exoplanet Survey Satellite (TESS)," *SPIE* 9143 (2014): 20R.

Rogers L. A., "*Most* 1.6 Earth-radius planets are not rocky," *ApJ* 801 (2015): 41.

Rowe, J. F., et al., "Validation of *Kepler's* Multiple Planet Candidates III: Light Curve Analysis and Announcement of Hundreds of New Multi-planet Systems," *ApJ* 784 (2014): 45.

Schwamb, M. E., et al., "Planet Hunters: A Transiting Circumbinary Planet in a Quadruple Star System," *ApJ* 768 (2013): 127.

Seader, S., et al., "Detection of Potential Transit Signals in 17 Quarters of *Kepler* Mission Data," *ApJS* 217 (2015): 18.

Sheets, H., and Deming, D., "Statistical Eclipses of Close-in Kepler Sub-Saturns," *ApJ* 794 (2014): 133.

Sotin, C., Grasset, O., and Mocquet, A., "Mass-radius Curve for Extrasolar Earth-like Planets and Ocean Planets," *Icarus* 191 (2007): 337.

Southworth, J., "Homogeneous Studies of Transiting Extrasolar Planets V: New Results for 38 Planets," *MNRAS* 426 (2012): 1291.

Udry, S., and Santos N. C., "Statistical properties of exoplanets," *Annu. Rev. Astron. Astrophys.* 45 (2007): 397.

Valencia, D., O'Connel, R. J., Sasselov, D., "Internal Structure of Massive Terrestrial Planets," *Icarus* 181 (2006): 545–54.

Welsh, W., et al., "The Discovery of Ellipsoidal Variations in the *Kepler* Light Curve of HAT-P-7," *ApJL* 713 (2010): L145–9.

Welsh, W., et al., "Recent *Kepler* Results on Circumbinary Planets," in *Formation, Detection, and Characterization of Extrasolar Habitable Planets*, ed. N. Haghighipour, IAUS Sym #293 Proceedings (2012).

Wolszczan, A., and Frail, D. A., "A Planetary System around the Millisecond Pulsar PSR1257 + 12," *Nature* 355 (1992): 145.

Wright, J. T., et al., "The Search for Extraterrestrial Civilizations with Large Energy Supplies IV: The Signatures and Information Content of Transiting Megastructures," *ApJ* 816 (2016): 17.

Xue, Y., and Suto, Y., "Difficulty in Formation of Counter-orbiting Hot Jupiters from Near-coplanar Hierarchical Triple Systems: A Sub-stellar Perturber," *The Astrophysical Journal* 820 (2016): 55.